THE JOURNAL OF BIOLOGICAL CHEMISTRY VOL. 282, NO. 17, pp. 12765–12772, April 27, 2007

Molecular Analysis of the Role of Tyrosine 224 in the Active Site of *Streptomyces coelicolor* RppA, a Bacterial Type III Polyketide Synthase*[S]

Received for publication, January 16, 2007, and in revised form, February 28, 2007 Published, JBC Papers in Press, March 1, 2007, DOI 10.1074/jbc.M700393200

Shengying Li[‡§], Sabine Grüschow[‡§], Jonathan S. Dordick[¶], and David H. Sherman[‡§‖1]**

*From the [‡]Life Sciences Institute and Departments of [§]Medicinal Chemistry, [‖]Chemistry, and **Microbiology & Immunology, University of Michigan, Ann Arbor, Michigan 48109 and the [¶]Department of Chemical and Biological Engineering, Rensselaer Polytechnic Institute, Troy, New York 12180*

Streptomyces coelicolor **RppA (Sc-RppA), a bacterial type III polyketide synthase, utilizes malonyl-CoA as both starter and extender unit substrate to form 1,3,6,8-tetrahydroxynaphthalene (THN) (therefore RppA is also known as THN synthase (THNS)). The significance of the active site Tyr^{224} for substrate specificity has been established previously, and its aromatic ring is believed to be essential for RppA to select malonyl-CoA as starter unit. Herein, we describe a series of Tyr^{224} mutants of Sc-RppA including Y224F, Y224L, Y224C, Y224M, and Y224A that were able to catalyze a physiological assembly of THN, albeit with lower efficiency, challenging the necessity for the Tyr^{224} aromatic ring. Steady-state kinetics and radioactive substrate binding analysis of the mutant enzymes corroborated these unexpected results. Functional examination of the Tyr^{224} series of RppA mutants using diverse unnatural acyl-CoA substrates revealed the unique role of malonyl-CoA as starter unit substrate for RppA, leading to the development of a novel steric-electronic constraint model.**

Type III polyketide synthases (PKSs)[2] represent the structurally simplest member of the PKS superfamily (1, 2), which also consists of the giant modular multifunctional type I PKS (3, 4) and the discrete multienzyme type II PKS (5, 6). Since the discovery of the first type III PKS, chalcone synthase (CHS), in the 1970s (7), a growing number of type III PKSs have been identified in plants (8–10), bacteria (11–13), and fungi (14). All members of the family characterized to date share some common structural and mechanistic features (2) including a homodimeric architecture, similar subunit molecular mass (40–47 kDa), analogous active site structure, a conserved Cys-His-Asn catalytic triad (thus a common reaction mechanism), and the utilization of acyl-coenzyme A (acyl-CoA) thioesters as substrates instead of the acyl-carrier protein-linked substrates employed by type I and II PKSs. To diversify polyketide product output, type III PKSs have evolved to use a wide range of natural acyl-CoA substrates. For example, the plant type III PKSs, which share 60–95% amino acid identity (2), utilize a variety of different substrates ranging from aliphatic-CoA to aromatic-CoA, from small acetyl-CoA (2-pyrone synthase in *Gerbera hybrida*) (15) to bulky *p*-coumaroyl-CoA (*Medicago sativa* CHS) (16) or from the polar malonyl-CoA (*Aloe arborescens* pentaketide chromone synthase) (17) to the relatively nonpolar isovaleroyl-CoA (*Humulus lupulus* phlorisovalerophenone synthase) (18).

Interestingly, the more divergent bacterial type III PKSs (with as low as 20% amino acid identity) utilize a much narrower pool of natural acyl-CoA substrates than their relatives in plants (1, 2). Specifically, RppA from either *Streptomyces coelicolor* or *Streptomyces griseus* (19, 20), *Pseudomonas fluorescens* PhlD (21), and *Amycolatopsis mediterranei* DpgA (22, 23) coincidentally employ malonyl-CoA as their physiological starter unit, although alternative starter substrates are known to be accepted by these enzymes (24, 25). Such limited physiological substrate specificity may be misleading because of a paucity of information on functionally identified bacterial type III PKSs (12, 26, 27), a reflection of the short period of time since their discovery. Alternatively, the more limited substrate variability of bacterial type III PKSs might reflect convergent evolution within this family resulting from the more limited availability of acyl-CoA building blocks in prokaryotes compared with eukaryotes. With respect to the limited "building block" diversity in bacteria, it is intriguing that such seemingly divergent bacterial type III PKSs utilize a common starter unit. Understanding the convergence of bacterial type III PKS structure and function could provide important insights into substrate preferences and specificity, potentially enabling expansion of the repertoire of unnatural substrates and thus the creation of functionally diverse and novel natural products.

S. griseus RppA (Sg-RppA) has provided substantial fundamental information about the catalytic properties of the type III PKS subfamily as the first functionally characterized bacterial enzyme of its class (19, 28). The physiological reaction (Fig. 1*A*) is initiated by loading a malonyl-CoA molecule covalently onto

* This work was supported by the Defense Advanced Research Projects Agency (DARPA), National Science Foundation (NSF) Grant BES-0118926, and the J. G. Searle professorship (to D. H. S.) and by NSF Grant BES-0118820 and National Institutes of Health Grant M66712 (to J. S. D.). The costs of publication of this article were defrayed in part by the payment of page charges. This article must therefore be hereby marked "*advertisement*" in accordance with 18 U.S.C. Section 1734 solely to indicate this fact.

[S] The on-line version of this article (available at http://www.jbc.org) contains supplemental Figs. S1 and S2.

[1] To whom correspondence should be addressed: Life Sciences Inst. and Dept. of Medicinal Chemistry, University of Michigan, Ann Arbor, MI 48109-2216. Tel.: 734-615-9907; Fax: 734-615-3641; E-mail: davidhs@umich.edu.

[2] The abbreviations used are: PKS, polyketide synthase; acyl-CoA, acyl coenzyme A; WT, wild type; Sc-RppA, *S. coelicolor* RppA; Sg-RppA, *S. griseus* RppA; THN, 1,3,6,8-tetrahydroxynaphthalene; TAL, triacetic acid lactone; CHS, chalcone synthase; HPLC, high pressure liquid chromatography.

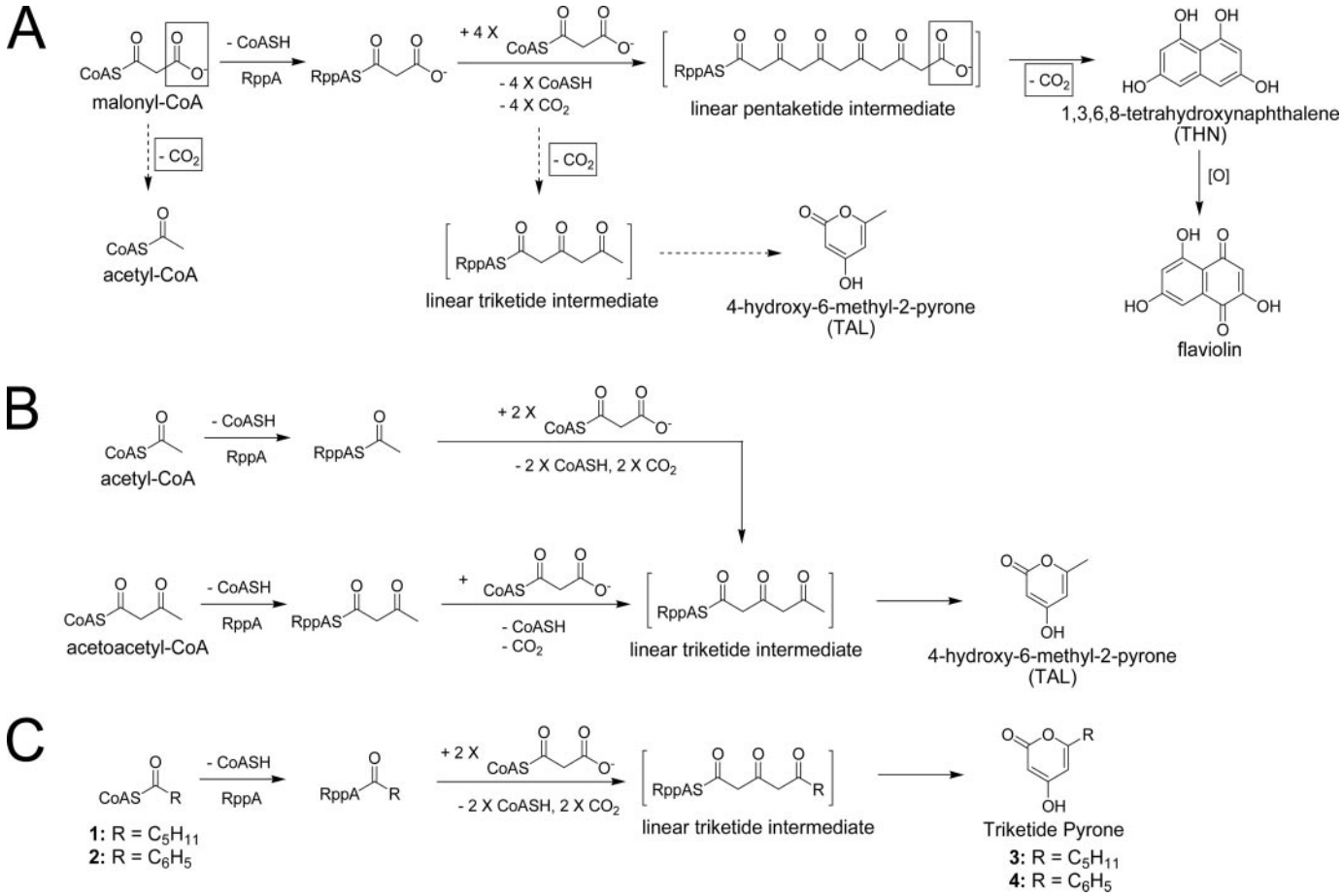

FIGURE 1. **Reactions catalyzed by Sc-RppA.** *A*, malonyl-CoA-initiated reaction. The *dashed arrows* indicate reactions leading to derailed products, and the *boxed* moieties derive from the starter malonyl-CoA. *B*, acetyl-CoA and acetoacetyl-CoA-primed reactions. *C*, hexanoyl-CoA **1**- and benzoyl-CoA **2**-initiated reactions.

the catalytic Cys^{138} of the RppA polypeptide. Four acetyl-CoA extender units, generated from decarboxylation of malonyl-CoA, are then added sequentially to the elongating linear intermediate via Claisen condensation. Finally, the linear pentaketide intermediate is cyclized and aromatized to form 1,3,6,8-tetrahydroxynaphthalene (THN), although the mechanism of this termination step remains unclear. During growth of the linear polyketide intermediate, the terminal carboxyl group is presumably derived from the starter malonyl-CoA and is prevented from premature decarboxylation, which would result in derailment to acetyl-CoA or triacetic acid lactone (TAL; 4-hydroxy-6-methyl-2-pyrone) via intramolecular cyclization (Fig. 1*A*).

The importance of the active site Tyr^{224} residue in the first step of this reaction relating to starter unit specificity of Sg-RppA was previously identified through analyzing the ability of a series of mutants to produce THN (28). It was revealed that although the aromatic amino acid Trp or Phe replacement of Tyr^{224} is tolerated by Sg-RppA, other Tyr^{224} mutants including Y224L, Y224G, and Y224C are inactive. In contrast, these mutants are functional when hexanoyl-CoA or phenylacetyl-CoA is presented as a nonphysiological starter unit. On the basis of these observations, Funa *et al.* (28) proposed that Tyr^{224} in Sg-RppA is critical for starter unit (malonyl-CoA) selection. Interestingly, this Tyr residue is also conserved in DpgA and PhlD (supplemental Fig. S1), the other two functionally identified bacterial type III PKSs that utilize malonyl-CoA as the physiological starter unit. The function of Tyr^{224} in RppA was further discussed by Austin *et al.* (29) upon analyzing the crystal structure of *S. coelicolor* RppA (Sc-RppA), which is the closest relative to *S. griseus* RppA (67% amino acid identity) and catalyzes an identical series of reactions. In the 2.22 Å crystal structure, Tyr^{224} was found at the surface of the active site pocket of Sc-RppA (8.5 Å away from the catalytic Cys^{138}) and was believed to exert a horizontal steric constraint to the first entering malonyl-CoA through its bulky side chain, thereby positioning the starter unit at a favorable location (near the catalytic Cys^{138}) by limiting conformational freedom. Accordingly, the small amino acid Gly cannot play a similar role. Thus, when the position corresponding to Tyr^{224} is occupied by a Gly in CHS (supplemental Fig. S1), this plant type III PKS cannot use malonyl-CoA as a starter unit. It is evident that the Gly residue provides additional space for accommodating the bulky substrate *p*-coumaroyl-CoA (30, 31). This volume-modulating model for substrate specificity is currently well accepted (2, 31). However, it has remained unclear how inactive Tyr^{224} mutants (Y224L, Y224G, and Y224C) enable selection of unnatural acyl-CoAs as the starter unit substrate in Sg-RppA.

Although Sc-RppA and Sg-RppA are highly homologous and possess nearly identical active site compositions, Sc-RppA was

reported to have higher tolerance toward unnatural acyl-CoA starter units than Sg-RppA (25). For example, both acetyl-CoA and benzoyl-CoA were substrates for the Sc-RppA yet were not accepted by Sg-RppA (24). Thus, considering the broader flexibility, together with the corresponding x-ray crystal structure, Sc-RppA represents a compelling target for the study of substrate specificity because of its ability to accept various unnatural substrates, especially acyl-CoAs, which cannot be utilized by Sg-RppA.

In the current study we generated a series of point mutations at the Tyr^{224} residue in Sc-RppA and compared the resulting product profile to the wild type (WT) enzyme. To elucidate further how this residue determines substrate selectivity, acetoacetyl-CoA, acetyl-CoA, hexanoyl-CoA, and benzoyl-CoA, which, respectively, represent the spectrum of similar, smaller, and larger (aliphatic hexanoyl-CoA and aromatic benzoyl-CoA) substrates compared with malonyl-CoA, were examined as unnatural acyl-CoA starter units by both WT and Tyr^{224} mutant forms of Sc-RppAs. Moreover, the correlation between substrate loading and product formation of these enzymes was examined by radioactive substrate binding analysis. This investigation confirmed that the inability of Tyr^{224} mutants to synthesize THN results from failure to load malonyl-CoA onto the catalytic Cys residue as opposed to failure of subsequent chain elongation, cyclization, or product release steps.

EXPERIMENTAL PROCEDURES

S. coelicolor RppA Gene Cloning—Genomic DNA was prepared from *S. coelicolor* A3 (2) using a Wizard genomic DNA purification kit (Promega). The Sc-RppA gene was amplified by PCR under standard conditions with a pair of primers as follows: forward, 5′-AATCATATGGCGACTTTGTGC-3′ (the underlined bases represent the introduced NdeI site for further cloning); reverse, 5′-AATAAGCTTTCATGCCTGCCTGCCTCACCC-3′ (the underlined letters indicate a HindIII restriction site for later cloning). The full-length cDNA encoding Sc-RppA was rescued by double digestion of NdeI and HindIII. The fragment containing Sc-RppA gene was ligated into previously NdeI/HindIII-digested pET-28b(+) (Novagen) to generate the recombinant plasmid pET-28b(+)-Sc-RppA. This construct was then transformed into *Escherichia coli* BL21(DE3) for protein overexpression. The accuracy of the inserted Sc-RppA gene was confirmed by nucleotide sequencing.

Site-directed Mutagenesis, Protein Overexpression, and Purification—Site-directed mutagenesis was performed according to the QuikChange (Stratagene) protocol with pET-28b(+)-Sc-RppA as template. The PCR-amplified plasmids containing mutations were verified by DNA sequencing and then directly used for transforming the protein overexpression strain *E. coli* BL21(DE3). The resulting transformants were grown at 37 °C overnight in Luria broth containing 50 μg/ml kanamycin, and 10 ml of culture was used to inoculate 1 liter of Terrific Broth containing 50 μg/ml of kanamycin. The Terrific Broth culture was incubated at 37 °C for 3~4 h until A_{600} reached 0.6–1.0. Then, gene overexpression was induced by adding isopropyl-β-D-thiogalactopyranoside to a final concentration of 0.1 mM and cultured at 18 °C overnight. The culture was centrifuged at 4,000 × *g* for 10 min to collect cells. The freeze-thaw cell pellet was resuspended in 40 ml of lysis buffer (250 mM NaCl, 50 mM NaH_2PO_4, 10 mM imidazole, 20% glycerol, pH 7.9), and the cell lysate was prepared by lysozyme digestion at 1 mg/ml for 30 min with subsequent sonication. Cell debris was removed by centrifugation at 15,000 × *g* for 30 min, and the soluble fraction was mixed with 2 ml nickel-nitrilotriacetic acid-agarose (Qiagen) for 1 h at 4 °C. The slurry was loaded onto an empty column. The column was then washed stepwise with 20 ml of lysis buffer and 40–60 ml of wash buffer (250 mM NaCl, 50 mM NaH_2PO_4, 40 mM imidazole, 20% glycerol, pH 7.9). The His_6 tag bound proteins were eluted with elution buffer (250 mM NaCl, 50 mM NaH_2PO_4, 200 mM imidazole, 20% glycerol, pH 7.9). The target protein was further purified and concentrated with YM-10 centrifuge filters (Amicon). Finally, the elution buffer was exchanged for storage buffer (250 mM NaCl, 50 mM NaH_2PO_4, 20% glycerol, pH 7.4) with a PD-10 column (GE Healthcare), and the resulting product concentrations were measured by Bio-Rad protein assay kit using bovine serum albumin as standard. Purity and molecular mass were examined by standard SDS-PAGE analysis.

RppA Enzymatic Assay—The standard assay containing 50 mM sodium phosphate (pH 7.4), 0.2 mM acyl-CoA starter, and 3 μM WT or mutant RppA in a total volume of 100 μl was initiated by adding malonyl-CoA to a final concentration of 0.5 mM and was quenched with the addition of 10 μl of 6 M HCl after incubation at 30 °C for 1 h. Small amounts of enzyme were removed by centrifugation at 16,100 × *g* for 10 min. The supernatant was used directly as the sample for HPLC analysis. Reverse-phase HPLC conditions were as follows, using an XBridge C18 5-μm column (4.6 × 250 mm): the mobile phase for the malonyl-CoA-, acetyl-CoA-, and acetoacetyl-CoA-primed reaction was linear from 5 to 35% *B* (*A* = deionized water + 0.1% trifluoroacetic acid; *B* = acetonitrile + 0.1% trifluoroacetic acid) over 20 min, and the mobile phase for the hexanoyl-CoA- and benzoyl-CoA-primed reaction was linear from 20 to 70% *B* over 20 min; the UV detection wavelength was 280 nm for the malonyl-CoA-, acetyl-CoA-, acetoacetyl-CoA-, and hexanoyl-CoA-primed reactions and 320 nm for the benzoyl-CoA primed reaction, at a flow rate of 0.8 ml/min. The peak identity in HPLC trace was determined by mass spectrometry and comparison with authentic compounds regarding HPLC retention time and UV spectrum.

Enzyme Kinetics—We exploited the reported coefficient constant for THN at 340 nm (ϵ = 18,000) (20) to obtain the steady-state kinetic parameters using a spectrophotometric method. The standard reaction buffered with 100 mM Tris-HCl (pH 7.5) containing the appropriate concentration of WT or mutant RppA in a total volume of 400 μl was initiated by adding a series of concentrations of malonyl-CoA ranging from 1 to 100 μM and was immediately monitored with a UV-visible spectrophotometer 300 Bio (Cary) at 30 °C. The initial velocity of THN accumulation was deduced from the absorbance curve within the linear range. All measurements were determined in triplicate, and velocities determined under different malonyl-CoA concentrations were fit to the Michaelis-Menten equation to calculate the kinetic constants k_{cat} and K_m.

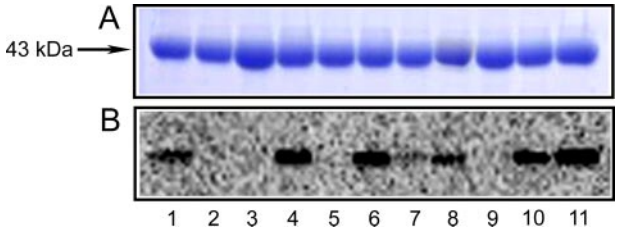

FIGURE 2. **Radioactive substrate binding analysis of WT and mutant Sc-RppAs with [2-^{14}C]malonyl-CoA as radioactive label.** *A*, Coomassie blue-stained 15% SDS-polyacrylamide gel. *B*, autoradiograph of the dried SDS-polyacrylamide gel. *Lanes*: *1*, WT Sc-RppA; *2*, C138A; *3*, C138S; *4*, Y224L; *5*, Y224G; *6*, Y224A; *7*, Y224S; *8*, Y224M; *9*, Y224H; *10*, Y224C; *11*, Y224F.

Radioactive Substrate Binding Assay—The optimized reaction contained 50 mM HEPES buffer (pH 7.4), 50 μM [2-^{14}C]malonyl-CoA (55 mCi/mmol) and 15.0 μM WT or mutant enzymes in a total volume of 25 μl. Reactions were quenched by the addition of 25 μl of 2× SDS gel loading dye after a 5-min incubation at 30 °C. 10 μl of each reaction mixture was analyzed by SDS-PAGE (15%). After staining, destaining, and drying the protein gel on filter papers, the radioactivity bound to the protein was determined by autoradiography following a 4-day exposure using a PhosphorImager (Amersham Biosciences).

RESULTS

WT and Mutant RppA Overexpression and Purification—The substitution of Leu, Gly, Ala, Ser, Met, His, Cys, and Phe for Tyr^{224} was conducted to explore the effect of locally modifying steric and electronic/polarity properties on starter unit loading. The WT enzyme and Tyr^{224} series of RppA mutants were overexpressed in *E. coli* BL21(DE3) and purified to homogeneity. As shown by SDS-PAGE (Fig. 2*A*), the monomer of each purified protein migrated with a molecular mass of ~43 kDa. Interestingly, previously reported purification efforts of the corresponding Sg-RppA Y224S and Y224H mutants were unsuccessful due to insolubility (28). This discrepancy might result from an intrinsic difference between these two RppAs, the type of cloning system or purification procedure used, or other variables. Nevertheless, each of the Sc-RppA mutant enzymes was expressed as a soluble polypeptide to enable more detailed analysis.

Mutant Activity Analysis—Using WT Sc-RppA as a positive control and the catalytic Cys mutants C138A and C138S as negative controls, we first examined the activities of the Tyr^{224} mutants of Sc-RppA to utilize malonyl-CoA. The reactivity of each mutant was assayed by measuring the amount of accumulated THN by HPLC analysis. Because authentic THN is not isolable due to its rapid conversion to flaviolin (Fig. 1*A*) (19), we elected to deduce the relative yield of THN by integration of the HPLC peak area using WT RppA enzyme as a reference. As shown in Fig. 3*A*, among the eight Tyr^{224} mutants, Y224G, Y224S, and Y224H were unable to catalyze assembly of THN (as negative controls). The inactivity of Y224G is not surprising because Y224G of Sg-RppA was also an inactive mutant (28). For Y224S (whose counterpart in Sg-RppA was insoluble), this inactivation could be attributed to horizontal expansion of the active site through replacement of a smaller side chain. However, it is currently unclear why the RppA Y224H mutant cannot synthesize THN from malonyl-CoA considering the size of the His side chain. In contrast, Y224F, Y224L, Y224C, Y224M, and Y224A retained 71, 67, 48, 16, and 3% of its activity, respectively, relative to WT Sc-RppA. A previous study reported Y224L, Y224C, and Y224A (but not Y224F) from Sg-RppA to be inactive toward malonyl-CoA (28). To further probe the basis for this discrepancy, we prepared WT Sg-RppA (from *S. griseus* NRRL B-2682) and its corresponding Y224L mutant to compare their ability to generate THN. Surprisingly, this Y224L mutant produced an ~50% level of THN compared with WT Sg-RppA (supplemental Fig. S2). Therefore, this (re)examination of Y224L mutants indicates that the Leu replacement retains significant catalytic activity in both Sc-RppA and Sg-RppA.

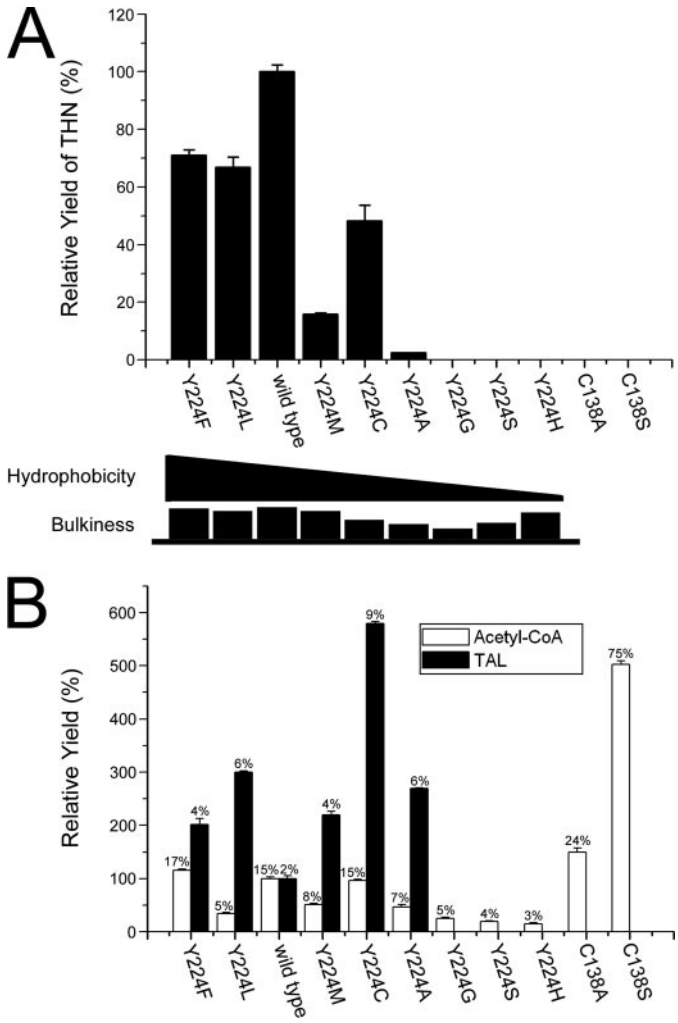

FIGURE 3. **The product profile of malonyl-CoA-initiated reactions catalyzed by WT or mutant Sc-RppA.** The product profile of Sc-RppA catalyzed reactions was analyzed by HPLC at 280 nm. All reactions were duplicated and the relative yields calculated from the integrated peak area of the HPLC trace using WT enzyme as reference (100%). *A*, the *upper portion* shows the THN production profile. The *lower portion* displays the amino acid hydrophobicity tendency and bulkiness (van der Waals volume). *B*, profile of the derailment products acetyl-CoA and TAL. The percentage of incorporated malonyl-CoA is shown *above* each *bar*.

As described, in addition to the major product THN, a low level of malonyl-CoA would be incorporated into two other derailment products (acetyl-CoA and TAL) because of premature decarboxylation of the oligoketide chain (Fig. 1*A*).

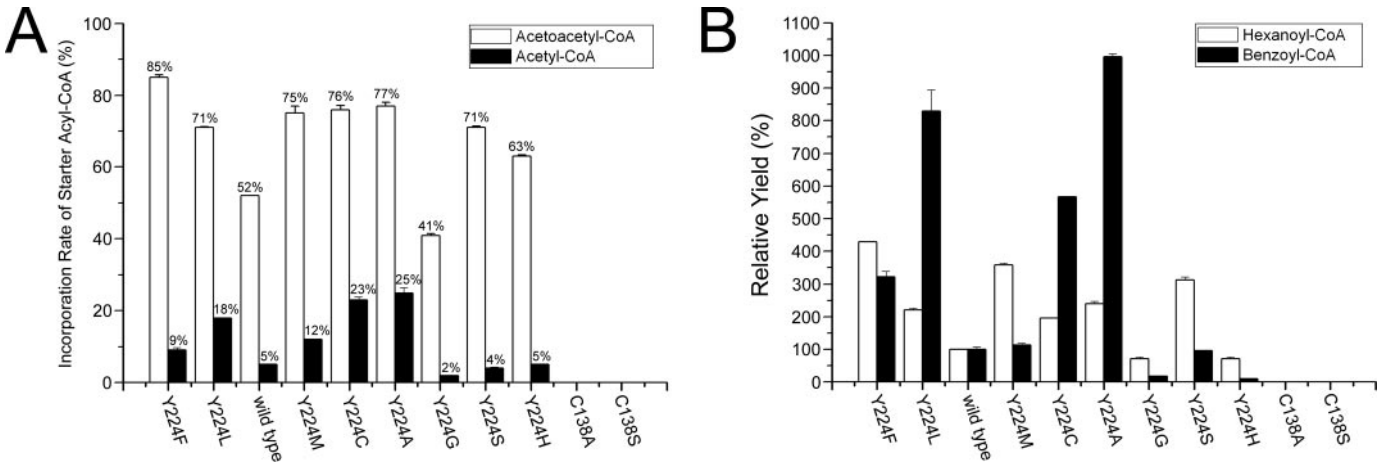

FIGURE 4. **The product profile of diverse acyl-CoA-initiated reactions catalyzed by WT or mutant Sc-RppA.** *A*, acetoacetyl-CoA- and acetyl-CoA-initiated reactions. Production of TAL from either acetoacetyl-CoA or acetyl-CoA was monitored at UV_{280} in duplicate. The *numbers* above each bar indicate the percentage of incorporated starter unit substrates that were calculated based on absolute yields of TAL. *B*, hexanoyl-CoA- and benzoyl-CoA-primed reactions. The relative yields of hexanoyl triketide pyrone **3** and benzoyl triketide pyrone **4** were measured at 280 and 320 nm, respectively, by using WT enzyme as reference (100%). All reactions were duplicated.

Because the synthesis of these by-products might provide new mechanistic insights into this type III PKS, we extended our analysis to the production of acetyl-CoA and TAL (Fig. 3*B*). Specifically, the five partially active mutants (Y224F, Y224L, Y224M, Y224C, and Y224A) accumulated corresponding increased levels of TAL relative to WT Sc-RppA, suggesting the dual function of Tyr^{224}. In addition to the contribution to substrate specificity determination, Tyr^{224} potentially is able to influence the extent of polyketide chain elongation, thus affecting the partitioning of TAL formation. On the contrary, the mutants that lack an ability to synthesize THN were not able to accumulate TAL. This clearly indicates that the biochemical effect from the Tyr mutation occurs prior to formation of the triketide intermediate. Moreover, no CoASH was released (data not shown) strongly suggesting that these inactive mutants cannot load malonyl-CoA. Significantly, all Tyr^{224} mutants (together with the negative controls) were capable of producing acetyl-CoA, which indicates that this residue has no significant influence on the decarboxylative activity of Sc-RppA. It was also noteworthy that the decarboxylative activities of both the C138A and C138S mutants were significantly higher than WT enzyme. Approximately, 24 and 75% of the malonyl-CoA substrate was converted to the terminal metabolite acetyl-CoA in the C138A and C138S mutant forms of Sc-RppA, respectively. A similar observation was reported previously in the C138A and C138S mutant forms of DpgA (23).

Next, using acetoacetyl-CoA or acetyl-CoA as the starter substrate and malonyl-CoA as the extender unit, we observed that all Tyr^{224} mutants (except for the negative controls C138A and C138S) were able to produce TAL from either acetoacetyl-CoA or acetyl-CoA (Fig. 4*A*) via intramolecular lactonization of the triketide linear chain elongation intermediate (Fig. 1*B*). The mutants with partial ability to generate THN produced significantly higher levels of TAL from either acetoacetyl-CoA or acetyl-CoA compared with WT Sc-RppA. We surmise that this was a result of the decreased loading efficiency of malonyl-CoA as a starter unit, resulting in a greater propensity for loading of alternative acyl-CoAs due to increased availability of the active site toward unnatural substrates. Moreover, these partially active Tyr^{224} mutants still accumulated THN, leading to a production profile similar to that shown in Fig. 3*A* (data not shown), although the corresponding yields were lower because of competition of unnatural acyl-CoA against malonyl-CoA as starter unit. More importantly, the inactive Tyr^{224} mutants including Y224H, Y224S, and Y224G were capable of accepting acetoacetyl-CoA and acetyl-CoA, resulting in a substantial accumulation of TAL with an incorporation rate ranging from 41 to 71% and 2 to 5% for acetoacetyl-CoA and acetyl-CoA, respectively. It was evident that the incorporation rate of acetoacetyl-CoA (41–85%) was significantly higher than acetyl-CoA (2–25%). For instance, by calculating the absolute yield of TAL using authentic material as a standard, we determined that 52% of acetoacetyl-CoA was converted to TAL by WT Sc-RppA, whereas only 5% of acetyl-CoA was found to be incorporated as TAL product (similar results were also observed in Sg-RppA (24) and PhlD (32)).

Finally, when we utilized hexanoyl-CoA or benzoyl-CoA as alternate starter units, the corresponding product profiles were comparable with those of acetoacetyl-CoA and acetyl-CoA generated by different Sc-RppAs (Fig. 4). Specifically, the products hexanoyl triketide pyrone **3** and benzoyl triketide pyrone **4** of Y224F, Y224L, Y224M, Y224C, and Y224A were observed in significantly higher amounts. With respect to the inactive Tyr^{224} mutants (Y224H, Y224S, Y224G), we demonstrated that they are also capable of synthesizing the corresponding triketide pyrones from hexanoyl-CoA and benzoyl-CoA, albeit at relatively low levels. In this analysis, however, we were not able to determine the incorporation rates due to lack of standard compounds.

Steady-state Kinetics of RppAs—The HPLC-based product profile analysis only provided qualitative information on the activities of Tyr^{224} mutants. To better understand the effect of each mutation, steady-state kinetic parameters based on overall THN formation of WT Sc-RppA and the Tyr^{224} mutants were determined (Table 1). The kinetics of WT Sc-RppA (k_{cat} = $1.33 \pm 0.05\ min^{-1}$, $K_m = 3.9 \pm 0.5\ \mu M$, $k_{cat}/K_m = 5739\ M^{-1} \cdot s^{-1}$

TABLE 1
Steady-state kinetic constants for THN production in WT and Tyr^{224} mutants of Sc-RppA and Sg-RppA

	Sc-RppA					Sg-RppA	
	WT	Y224F	Y224C	Y224L	Y224M	WT	Y224L
$k_{cat} \times 10^{-2}$ (min^{-1})	133.4 ± 4.8	110.0 ± 2.4	28.5 ± 0.8	24.6 ± 0.9	13.6 ± 0.7	284.2 ± 6.8	19.9 ± 0.6
K_m (μM)	3.9 ± 0.5	9.5 ± 0.3	12.0 ± 1.2	23.4 ± 2.0	17.1 ± 2.5	1.1 ± 0.2	11.1 ± 1.1
k_{cat}/K_m ($M^{-1}\cdot s^{-1}$)	5,739	1,930	396	175	133	44,476	298

were comparable with previous reports (20, 29). The mutants Y224F, Y224C, Y224L, and Y224M exhibited an ~2-, 13-, 32-, and 42-fold decrease in the k_{cat}/K_m value, respectively. These results provide direct support for the significance of Tyr^{224} on the substrate specificity of Sc-RppA. Concomitant with the increasing K_m value, the mutation of this Tyr residue also decreased the turnover number (k_{cat}), implicating its potential influence on the catalytic steps that follow substrate loading. Furthermore, we also determined the kinetic constants of WT Sg-RppA to be $k_{cat} = 2.84 \pm 0.07\ min^{-1}$, $K_m = 1.1 \pm 0.2\ \mu M$, $k_{cat}/K_m = 44476\ M^{-1}\cdot s^{-1}$, showing that Sg-RppA is more reactive toward malonyl-CoA than is Sc-RppA. Likewise, the Leu replacement of Tyr^{224} in Sg-RppA decreased the substrate specificity constant by 148-fold (Table 1).

Radioactive Substrate Binding to WT and Mutant Sc-RppAs—All previous data support the hypothesis that Tyr^{224} in the active site of RppA is involved in substrate specificity determination (28, 29, 31). However, direct evidence that Tyr^{224} facilitates covalent linkage of the first malonyl-CoA to Cys^{138} has been lacking. Previous work that revealed the inability of mutant Sg-RppAs to synthesize THN from malonyl-CoA could also result from successful loading but with an inability to catalyze polyketide chain extension, cyclization, or release of final product. To exclude these possibilities, radioactive malonyl-CoA was employed to detect the covalent radiolabel on WT or mutant RppA. Again, the Sc-RppA mutants C138A and C138S were included as negative controls. As expected, WT Sc-RppA and all Tyr^{224} mutants capable of synthesizing THN (Y224F, Y224L, Y224A, Y224M, and Y224C) were successfully radiolabeled through the covalent acylation of Cys^{138} with [2-^{14}C]malonyl-CoA (Fig. 2*B*). Together with negative controls, Y224H, Y224G, and Y224S were not labeled by radioactive malonyl-CoA. This substrate binding profile is consistent with the THN production profile (Fig. 3*A*), demonstrating the correlation between the starter substrate loading and product formation of Tyr^{224} mutants. Notably, compared with radiolabeled mutants, the radioactive intensity of acylated WT Sc-RppA was significantly lower. This might result from fast turnover of WT enzyme, thus leading to more released intermediates and products, both of which carry radioactivity. Moreover, WT and Y224L mutant Sg-RppA were also labeled by radioactive malonyl-CoA in a similar assay (data not shown).

DISCUSSION

Recently, the first ligand-free crystal structure of the bacterial type III PKS Sc-RppA was reported (29). However, until co-crystal structures bearing substrate, product, and chain elongation intermediates become available, the answers to three key mechanistic questions will remain outstanding. These include substrate specificity determination, polyketide chain length control, and mode of acyl chain cyclization. Dissection of these parameters currently depends primarily on biochemical analyses and modeling from CHS plant type III PKS. In the current study, we decided to revisit the role of Tyr^{224} in the active site of Sc-RppA and used site-directed mutagenesis to replace it with a series of alternative amino acid residues to probe its effect on starter unit specificity.

Jez *et al.* (30) observed, via comparison of x-ray crystal structures, that a point mutation at Gly^{256} (homologous to Tyr^{224} in RppA) of CHS does not cause significant alteration in the conformation of the polypeptide backbone. Based on the similarity between CHS and RppA, we reasoned that our series of Tyr^{224} substitutions would change only the local active site properties without inducing conformational changes. Surprisingly, our mutagenesis analysis results were significantly different from previous studies on the highly related type III PKS Sg-RppA (28). A series of Tyr^{224} mutants of Sc-RppA including Y224F, Y224C, Y224L, Y224M, and Y224A retained the ability to load malonyl-CoA and produce THN, although the catalytic activities were reduced. The current study demonstrates a higher tolerance toward certain amino acid changes at Tyr^{224} (28). Furthermore, we have demonstrated that the Leu replacement of Tyr^{224} in Sg-RppA does not eliminate malonyl-CoA starter unit selectivity (and hence THN formation). Interestingly, this positional tolerance was also observed recently in two plant type III PKSs, including *A. arborescens* pentaketide chromone synthase (17) and octaketide synthase (33), both of which harbor a Leu residue at the site corresponding to Tyr^{224} in RppA (supplemental Fig. S1) and utilize malonyl-CoA exclusively to initiate their physiological reactions. This demonstrates that plant type III PKSs employ a different strategy than bacterial enzymes to favor malonyl-CoA as the physiological starter unit. Quantitatively, the reported catalytic efficiencies (k_{cat}/K_m) of pentaketide chromone synthase and octaketide synthase with malonyl-CoA (k_{cat}/K_m = 104 and 16 $M^{-1}\cdot s^{-1}$ for pentaketide chromone synthase and octaketide synthase, respectively) (17, 33) are dramatically lower than those of the RppAs (k_{cat}/K_m = 5739 and 44476 $M^{-1}\cdot s^{-1}$ for Sc-RppA and Sc-RppA, respectively). The magnitude of the discrepancy suggests that Tyr might be the more highly optimized residue to favor malonyl-CoA with high efficiency. Correspondingly, we hypothesized that the Leu residue in these two plant type III PKSs might represent a compromise between malonyl-CoA incorporative efficiency and product complexity (or diversity), because the presence of a bulky residue at position 224 (such as Tyr) would presumably limit the number of chain extensions, thus impairing chemical diversity (30). In addition, *Rheum palmatum* aloesone synthase (34) and *G. hybrida* 2-pyrone synthase (15, 31) possessing Leu at the homologous position (supplemental Fig.

S1) can also generate products solely from malonyl-CoA, although their physiological starter unit is acetyl-CoA. This alternate conversion was previously thought to begin by decarboxylation of malonyl-CoA to generate acetyl-CoA (15). The studies reported here suggest that these two enzymes can directly incorporate malonyl-CoA, which competes directly with acetyl-CoA. Furthermore, studies showing that G256L and G256F mutants of CHS are able to produce TAL solely from malonyl-CoA could be interpreted similarly (30).

Prior to the work reported here, the conservation and presumed role of Tyr^{224} in bacterial type III PKSs indicated its importance in substrate specificity determination (28, 29). However, the hypothesis for its function has been focused on steric factors. The bulky aromatic side chain is believed to be essential for recruiting malonyl-CoA to the thiol group of catalytic Cys through a horizontal steric constriction for the malonyl-CoA starter unit. In this study, we obtained experimental data that could not be explained clearly by this model. First, together with the active Tyr^{224} mutants of Sc-RppA (Y224F, Y224C, Y224L, Y224M, and Y224A), all mutants (Y224G, Y224S, and Y224H) that were not able to use the physiological starter unit (malonyl-CoA) retained function toward diverse unnatural substrates including acetyl-CoA, acetoacetyl-CoA, hexanoyl-CoA, and benzoyl-CoA. Based on incorporation rates, all of these mutants displayed good activities toward acetoacetyl-CoA. This is not surprising considering that acetoacetyl-CoA is similar in size to malonyl-CoA. However, it remains unclear how Y224G, Y224S, and Y224H mutants are able to differentiate acetoacetyl-CoA from the isosteric malonyl-CoA. Second, we did not observe a correlation between the THN producing activity and the size of the replaced amino acid (Fig. 3*A*). Unexpectedly, the substitution of a series of nonconservative amino acids with significantly smaller side chains for Tyr^{224} (Y224C, Y224L, Y224M, and Y224A) was tolerated by Sc-RppA, which contradicts the described volume-modulating model (2, 31) for substrate specificity determination. For instance, in Y224C (one of the active mutants that continues to accommodate malonyl-CoA to produce THN), the small substituent Cys is isosteric to Ser; however the Ser mutation abrogated loading of the physiological starter unit (malonyl-CoA) based on radioactive substrate binding analysis. In contrast, modest modification of the active cavity volume by replacing Tyr^{224} with His completely disabled the malonyl-CoA loading ability of the mutant type III PKS. These results suggest that there might be an additional type of mechanism other than steric constraints that influences linkage of the first malonyl-CoA to the catalytic Cys. We initially considered that the most significant difference between acetoacetyl-CoA and malonyl-CoA was the terminal electronic property of the latter substrate. Based on observations reported here, it appears that the terminal negative charge of malonyl-CoA could be recognized by RppA. However, the polarity discrepancy is unable to be distinguished by the steric property of Tyr^{224} or other substituted residues at this position. Therefore, we propose that the hydrophobicity of Tyr^{224} could contribute to the preference for malonyl-CoA. Compared with other unnatural acyl-CoA substrates, malonyl-CoA carries a terminal negative charge at physiological pH (~7.5). Taking this electronic feature into account, when Tyr^{224} is replaced by a hydrophobic amino acid such as Leu, Cys, Met, or Ala (although missing the bulky side chain of Tyr), the hydrophobic interaction between the nonpolar side chain and the charged malonyl-CoA could limit the conformational freedom of this starter unit, thus decreasing the entropy penalty of covalent bond formation to active site Cys. However, hydrophobicity does not correlate perfectly with the THN productivity (Fig. 3*A*), indicating that steric factors remain important. Thus, the robustness of WT RppA likely derives from a combination of steric and electronic/polarity factors that favor malonyl-CoA. Additionally, the hydrophobic Y224A replacement generates only a slightly active mutant, possibly because of lack of steric effect to select the substrate. With respect to Y224H, the hydrophilic amino acid substitution might counteract the steric effect of its bulky side chain. Specifically, it is possible that the protonated His side chain could form an ionic interaction with the terminal negative charge of malonyl-CoA to prevent it from being linked to Cys^{138}.

Considering the current data, we propose that the ability of the malonyl-CoA-inactive mutants to accept unnatural acyl-CoAs that lack a terminal charge is governed by the hydrophobic interior of enzyme and the thermodynamically unfavorable conditions for delivering a formal charge there. Accordingly, an entropy compensation for substrate binding through limiting the conformational freedom of the substrate might be more stringent for the terminally charged malonyl-CoA than for other neutral unnatural acyl-CoAs.

In summary, we have demonstrated a surprising level of substrate tolerance involving a series of RppA Tyr^{224} mutations including both aromatic and hydrophobic amino acids with medium or large side chains. Both steric and electronic constraints exerted by Tyr^{224} in the active site are involved in facilitating the loading of the physiological substrate malonyl-CoA. In practical terms, re-engineering of plant and bacterial type III PKS to increase the preference for malonyl-CoA could be utilized to enable further product diversification. The identification of a number of active Tyr^{224} mutants with lower turnover numbers could provide potential candidates for subtle pre-steady-state kinetic studies, enzyme-linked intermediate trapping, or co-crystallization efforts. Moreover, the Tyr^{224} mutants that preferentially accept unnatural acyl-CoAs instead of malonyl-CoA could be applied for the production of novel pyrone products with higher yields.

REFERENCES

1. Moore, B. S., and Hopke, J. N. (2001) *Chembiochem* **2,** 35–38
2. Austin, M. B., and Noel, J. P. (2003) *Nat. Prod. Rep.* **20,** 79–110
3. Rawlings, B. J. (2000) *Nat. Prod. Rep.* **18,** 190–227
4. Katz, L., and Donadio, S. (1993) *Annu. Rev. Microbiol.* **47,** 875–912
5. Hutchinson, C. R., and Fujii, I. (1995) *Annu. Rev. Microbiol.* **49,** 201–238
6. Staunton, J., and Weissman, K. J. (2001) *Nat. Prod. Rep.* **18,** 380–416
7. Hahlbrock, K., and Kreuzaler, F. (1972) *Hoppe Seyler's Z. Physiol. Chem.* **353,** 1522–1526
8. Akiyama, T., Shibuya, M., Liu, H.-M., and Ebizuka Y. (1999) *Eur. J. Biochem.* **263,** 834–839
9. Schoppner, A., and H. Kindl, H. (1984) *J. Biol. Chem.*, 6806–6811
10. Helariutta, Y., Elomaa, P., Kotilainen, M., Griesbach, R. J., Schröder, J., and Teeri, T. H. (1995) *Plant Mol. Biol.* **28,** 47–60
11. Li, T.-L., Choroba, O. W., Hong, H., Williams, D. H., and Spencer, J. B.

(2001) *Chem. Commun.* (*Camb.*) **20,** 2156–2157
12. Sankaranarayanan, R., Saxena, P., Marathe, U. B., Gokhale, R. S., Shanmugam, V. M., and Rukmini, R. (2004) *Nat. Struct. Mol. Biol.* **11,** 894–900
13. Bangera, M. G., and Thomashow, L. S. (1999) *J. Bacteriol.* **181,** 3155–3163
14. Seshimea, Y., Juvvadia, P. R., Fujiib, I., and Kitamoto, K. (2005) *Biochem. Biophys. Res. Commun.* **331,** 253–260
15. Eckermann, S., Schröder, G., Schmidt, J., Strack, D., Edrada, R. A., Helariutta, Y., Elomaa, P., Kotilainen, M., Kilpeläinen, I., Proksch, P., Teeri, T. H., and Schröder, J. (1998) *Nature* **396,** 387–390
16. Heller, W., and Hahlbrock, K. (1980) *Arch. Biochem. Biophys.* **200,** 617–619
17. Abe, I., Utsumi, Y., Oguro, S., Morita, H., Sano, Y., and Noguchi, H. (2005) *J. Am. Chem. Soc.* **127,** 1362–1363
18. Paniego, N. B., Zuurbier, K. W., Fung, S.-Y., Van der Heijden, R., Scheffer, J. J., and Verpoorte, R. (1999) *Eur. J. Biochem.* **262,** 612–616
19. Funa, N., Ohnishi, Y., Fujii, I., Shibuya, M., Ebizuka, Y., and Horinouchi, S. (1999) *Nature* **400,** 897–899
20. Izumikawa, M., Shipley, P. R., Hopke, J. N., O'Hare, T., Xiang, L., Noel, J. P., and Moore, B. S. (2003) *J. Ind. Microbiol. Biotechnol.* **30,** 510–515
21. Achkar, J., Xian, M., Zhao, H., and Frost, J. W. (2005) *J. Am. Chem. Soc.* **127,** 5332–5333
22. Pfeifer, V., Nicholson, G. J., Ries, J., Recktenwald, J., Schefer, A. B., Shawky, R., Schroder, J., Wohlleben, W., and Pelzer, S. (2001) *J. Biol. Chem.* **276,** 38370–38377
23. Tseng, C. C., McLoughlin, S. M., Kelleher, N. L., and Walsh, C. T. (2004) *Biochemistry* **43,** 970–980
24. Funa, N., Ohnishi, Y., Ebizuka, Y., and Horinouchi, S. (2002) *J. Biol. Chem.* **277,** 4628–4635
25. Jeong, J.-C., Srinivasan, A., Grüschow, S., Bach, H., Sherman, D. H., and Dordick, J. S. (2005) *J. Am. Chem. Soc.* **127,** 64–65
26. Gross, F., Luniak, N., Perlova, O., Gaitatzis, N., Jenke-Kodama, H., Gerth, K., Daniela, G., Dittmann, E., and Müller, R. (2006) *Arch. Microbiol.* **185,** 28–38
27. Gerth, K., Pradella, S., Perlova, O., Beyer, S., and Müller, R. (2003) *J. Biotechnol.* **106,** 233–253
28. Funa, N., Ohnishi, Y., Ebizuka, Y., and Horinouchi, S. (2002) *Biochem. J.* **367,** 781–789
29. Austin, M. B., Izumikawa, M., Bowman, M. E., Udwary, D. W., Ferrer, J.-L., Moore, B. S., and Noel, J. P. (2004) *J. Biol. Chem.* **279,** 45162–45174
30. Jez, J. M., Bowman, M. E., and Noel, J. P. (2001) *Biochemistry* **40,** 14829–14838
31. Jez, J. M., Austin, M. B., Ferrer, J.-L., Bowman, M. E., Schroder, J., and Noel, J. P. (2000) *Chem. Biol.* **7,** 919–930
32. Zha, W., Rubin-Pitel, S. B., and Zhao, H. (2006) *J. Biol. Chem.* **281,** 32036–32047
33. Abe, I., Oguro, S., Utsumi, Y., Oguro, S., Sano, Y., and Noguchi, H. (2005) *J. Am. Chem. Soc.* **127,** 12709–12716
34. Abe, I., Utsumi, Y., Oguro, S., and Noguchi, H. (2004) *FEBS Lett.* **562,** 171–176

Molecular Analysis of the Role of Tyrosine 224 in the Active Site of *Streptomyces coelicolor* RppA, a Bacterial Type III Polyketide Synthase

Shengying Li, Sabine Grüschow, Jonathan S. Dordick and David H. Sherman

J. Biol. Chem. 2007, 282:12765-12772.
doi: 10.1074/jbc.M700393200 originally published online March 1, 2007